

*Jessica Baumgaertel is a senior at the University of Washington (UW) in Seattle majoring in physics and mathematics. During the summer of 2004, she held a Science Undergraduate Laboratory Internship at the Princeton Plasma Physics Laboratory in Princeton, NJ. Her project involved using linear simulations of drift waves to study microturbulence and stability of drift wave modes. This work was presented at the APS Division of Plasma Physics Annual Conference in 2004 and at the AAAS Annual Conference in 2005. At UW this year, Jessica worked on the Steady Inductive Helicity Injected Torus experiment in the Plasma Dynamics Group, studied various quantum mechanical paradoxes and elements of quantum computing, and was a teaching assistant for freshman physics classes. She will finish her B.S. degrees next year and hopes to then earn a PhD in physics.*

*Martha Redi is Principal Research Physicist at Princeton Plasma Physics Laboratory, Princeton University. She received a B.S. in physics from MIT (1964) and a Ph.D. in physics from Rutgers University (1969). She has published over 100 papers in superconductivity theory, theoretical biophysics, and oceanography as well as plasma physics. Since 1982 she has concentrated on computational plasma physics, testing theoretical ideas against experiment and planning new magnetic fusion devices. Her present interests center on astrophysical plasmas.*

## MARGINAL STABILITY STUDIES OF MICROTURBULENCE NEAR ITB ONSET ON ALCATOR C-MOD

JESSICA BAUMGAERTEL, M.H. REDI, R.V. BUDNY, D.C. McCUNE, W. DORLAND, AND C.L. FIORE

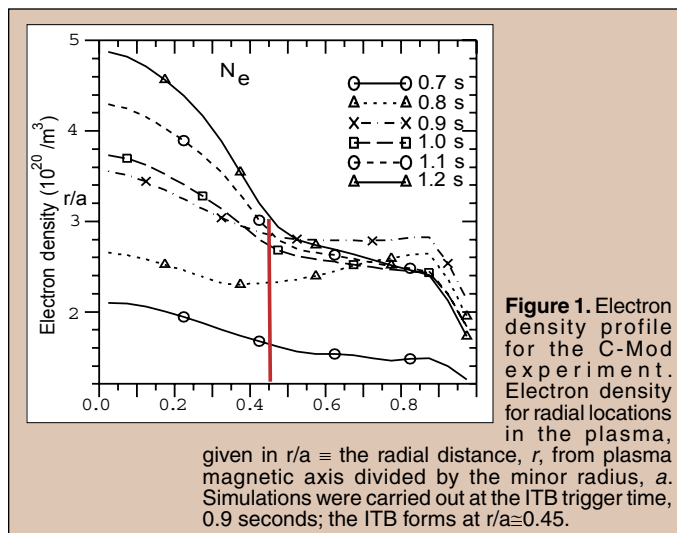
### ABSTRACT

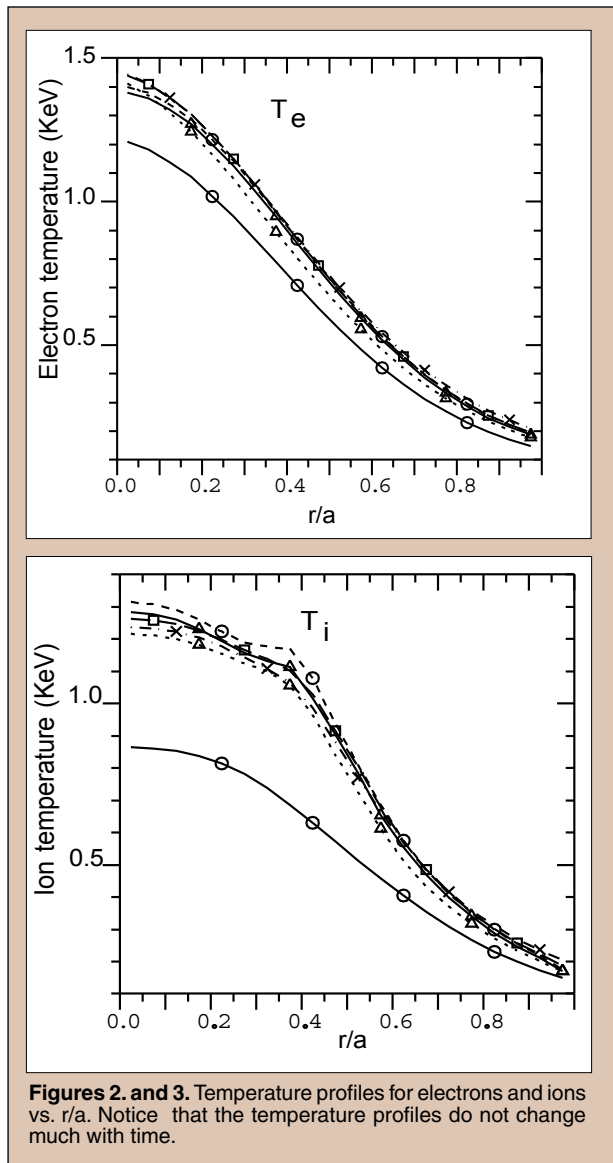
Insight into microturbulence and transport in tokamak plasmas is being sought using linear simulations of drift waves near the onset time of an internal transport barrier (ITB) on Alcator C-Mod. Microturbulence is likely generated by instabilities of drift waves and causes transport of heat and particles. This transport is studied because the containment of heat and particles is important for the achievement of practical nuclear fusion. We investigate nearness to marginal stability of ion temperature gradient (ITG) modes for conditions in the ITB region at the trigger time for ITB formation. Data from C-Mod, analyzed by TRANSP (a time dependent transport analysis code), is read by the code TRXPL and made into input files for the parallel gyrokinetic model code GS2. Temperature and density gradients in these input files are modified to produce new input files. Results from these simulations show a weak ITG instability in the barrier region at the time of onset, above marginal stability; the normalized critical temperature gradient is 80% of the experimental temperature gradient. The growth rate increases linearly above the critical value, with the spectrum of ITG modes remaining parabolic up to a multiplicative factor of 2. The effect of varying density gradients is found to be much weaker and causes the fastest growing drift mode to change from ITG to trapped electron mode character. Simulations were carried out on the NERSC IBM 6000 SP using 4 nodes, 16 processors per node. Predictive simulations were examined for converged instability after 10,000-50,000 timesteps in each case. Each simulation took approximately 30 minutes to complete on the IBM SP.

### INTRODUCTION

Insight into microturbulence and transport in tokamak plasmas is being sought using linear simulations of drift waves near the onset time of an internal transport barrier (ITB) on Alcator C-Mod [1]. Microturbulence is widely believed to be generated by drift wave instabilities causing transport of heat and particles. This transport is studied because the containment of heat and particles is important for the achievement of practical nuclear fusion. If transport was better understood, then it would be possible to design a better fusion reactor.

A tokamak is an experimental device which uses high magnetic fields to contain the charged particles of the plasma which may one day lead to energy from a practical fusion reactor. An ITB is a location





were undertaken to learn about the conditions in the plasma just before ITB formation, for possible ITB control.

A drift wave is an oscillation of plasma particle densities and currents and their electrostatic and electromagnetic fields. They are caused by particle drifts due to the electric and magnetic fields in the tokamak plasma, such as the  $\mathbf{E} \times \mathbf{B}$  drift of particles (Ref. [2], chapter 2). Charged particles move in a helical fashion around magnetic field lines, and in the presence of an electric field, they drift out of their helical orbits in a direction perpendicular to both  $\mathbf{E}$  and  $\mathbf{B}$ . Drifts can also arise from curvature of magnetic field lines and magnetic field gradients.

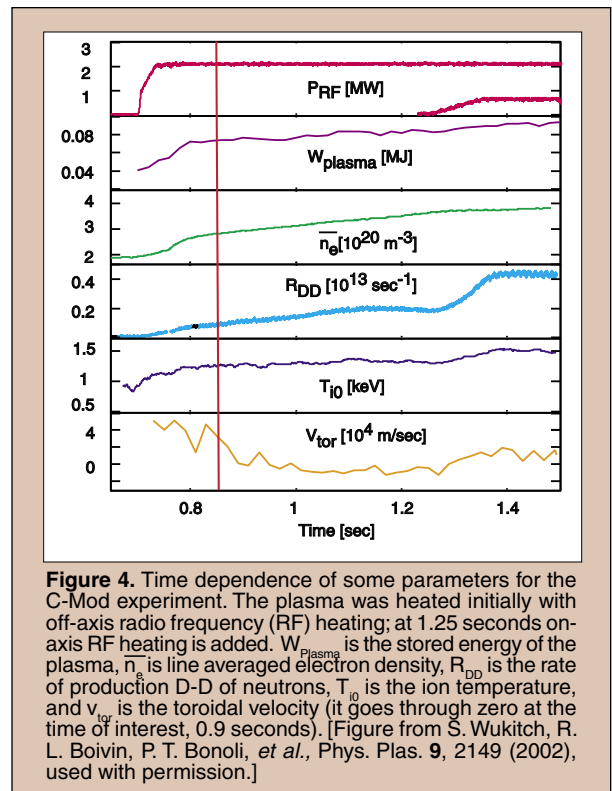
Components of the microturbulent electrostatic and electromagnetic fields may be written as  $\{S(\mathbf{k}, \omega)e^{i(\mathbf{k}\mathbf{x} - \omega t)}\}$ , each mode described by frequencies,  $\omega$ , and wave vectors,  $\mathbf{k}$ .  $k_{\perp}$  is perpendicular to the magnetic field line which wraps around a magnetic flux surface. Further details about drift wave physics may be found in reference [2], chapter 8.

Three types of drift waves are believed to affect plasma confinement: the ion temperature gradient (ITG) mode, the trapped electron mode (TEM), and the electron temperature gradient (ETG) mode. The normalized wave vectors,  $k_{\perp} \rho_s$ , of the ITG are in the range of  $k_{\perp} \rho_s \sim 0.1-0.8$ ; of the TEM,  $k_{\perp} \rho_s \sim 1-8$ ; and of the ETG,  $k_{\perp} \rho_s \sim 10-80$ , where  $\rho_s \equiv (\sqrt{m_i T_e})/eB$ . Because the ITG mode has the longest wavelength ( $\lambda = 2\pi/k$ ), it is most dangerous for causing plasma transport; such instabilities could cause a loss of heat or plasma on a larger scale than would the shorter wavelength modes. Therefore, we wish to see if our experiment is above or below marginal stability of the ITG (i.e., whether it has a positive or negative growth rate), and determine the critical temperature gradient so as to compare with standard models used in reactor design.

The experiment being studied is an off-axis radio frequency (RF) heated high performance plasma (H-mode) which develops an ITB near the time of 0.9 seconds (Figures 1-4) [3]. The ITB forms at a radius for which the ratio to the minor radius is  $r/a \approx 0.45$ . All of the simulations are based on data taken at the ITB trigger time, 0.9 seconds. Table I shows plasma parameters for the experiment.

## MATERIALS AND METHODS

To investigate the drift wave microturbulence, linear simulations of drift wave stability were carried out using the massively parallel code GS2 [4]. The time dependent transport analysis code TRANSP was used to analyze data from C-Mod and TRXPL was used to create GS2 input files from the TRANSP output [5]. These input files contain such information as the plasma equilibrium configuration, the plasma location of interest, and parameters for each of the plasma species, including density, temperature, gradients of the density and temperature, and collisionalities. The C-Mod



plasma was modeled with four species: electrons, deuterons, boron ions, and trace amounts of hydrogen ions. The neutral gas used was deuterium; the boron and hydrogen ions are present as impurities in the plasma.

GS2 solves the perturbed distribution function of the plasma particles, given by

$$(1) \quad f = f_0 + \left[ e_j \phi \frac{\partial f_0}{\partial K} + g \exp \left( i \frac{\mathbf{v}_\perp \times \mathbf{b} \cdot \mathbf{k}_\perp}{\omega_{cj}} \right) \right]$$

where  $g(\mu, K, x)$  satisfies the gyrokinetic equation:

$$(2)$$

$$\frac{\partial g}{\partial t} + \mathbf{v}_\parallel \mathbf{b} \cdot \nabla g + i \mathbf{k}_\perp \cdot \mathbf{v}_g g = - \left[ \omega \frac{\partial f_0}{\partial K} - \frac{\mathbf{b} \times \nabla f_0 \cdot \mathbf{k}_\perp}{\omega_{cj}} \right] \left[ J_0(z) e_j (\phi - v_\parallel A_\parallel) + \frac{2J_1(z)}{z} \mu B_\parallel \right]$$

$K$  is the kinetic energy of the particles,  $\phi$  and  $A_\parallel$  are perturbed potentials,  $\mathbf{b} = \mathbf{B}/|\mathbf{B}|$ ,  $e_j$  is the charge of the particle  $j$ ,  $\omega_{cj} = e_j B/m_j$  is the cyclotron frequency of particle  $j$ ,  $J_0(z)$  and  $J_1(z)$  are Bessel functions,  $v_\parallel$  and  $v_\perp$  are components of the particle velocity,  $\mathbf{k}_\perp$  is the perpendicular wave vector (inversely proportional to the wavelength of the drift wave),  $\mathbf{v}_g$  is the guiding center velocity, and  $z = k_\perp v_\perp / \omega_{cj}$ . (Reference [2], chapter 2.)

The simulations were carried out on the Department of Energy National Energy Research Scientific Computing Center's (NERSC) IBM 6000 SP, nicknamed Seaborg. Hundreds of linear stability simulations were carried out, scaling normalized density and temperature gradients for each case. Each simulation used 4 nodes, 16 processors per node and took approximately 30 minutes to complete on the IBM SP.

GS2 simulations yield growth rates,  $\gamma$ , and real frequencies,  $\omega$ , for each wave vector of the simulated drift wave. These values were examined for converged instability (positive  $\gamma$  and corresponding  $\omega$ ) after 10,000-50,000 time steps in each case, and plotted with EXCEL. GS2 also calculates eigenfunctions of the electrostatic and electromagnetic fields for each wave vector.

## RESULTS

### A. Instabilities in Three Regions of the Plasma

For each run, EXCEL was used to plot the growth rates and real frequencies as functions of normalized wave vectors,  $k_\perp \rho_s$ . Wave vectors, which correspond to the ITG, TEM, and ETG mode drift waves, were plotted for three locations in the plasma: the plasma core, the ITB region, and outside of the ITB. Negative growth rates denote damped modes ( $e^{-\gamma t}$ ) and are set to zero in the plots. Figures 5 and 7 show the growth rates,  $\gamma$ , and the frequencies,  $\omega$ , as a function of wave vector,  $k_\perp \rho_s$ , for all three drift wave mode ranges, while Figure 6 shows  $\gamma$  for only the ITG range of  $k_\perp \rho_s$  [6]. It was found that there are positive growth rates for ITG and ETG modes at and outside of the ITB, but no strongly unstable modes inside the plasma core. The real frequencies describe the mode rotation direction around the field line and are typically positive when the drift wave is an ITG mode, and negative for TEM and ETG modes.

### B. At the ITB Region: Temperature Gradient Scaling

Next, the ITG range of wave vectors at the ITB region was considered and the normalized temperature gradients ( $a\nabla T/T$ , Table I) of each of the plasma species were scaled in order to obtain the dependence of growth rate on temperature gradient. The gradient was varied by factors of 0.1 to 10. Figure 8 shows  $\gamma$  versus  $k_\perp \rho_s$  for each case. From this, the maximum growth rate for each case was plotted as a function of the scaling factor on the normalized temperature gradient (Figure 10). The real frequencies,  $\omega$ , versus  $k_\perp \rho_s$  are shown in Figure 9, and the real frequency corresponding to the maximum growth rate per run is plotted as a function of scaling factor in Figure 11.

### C. At the ITB Region: Density Gradient Scaling

Next, the normalized density gradients ( $a\nabla n/n$ , Table I) of the plasma species were scaled to examine the ITG growth rate dependence on normalized density gradient. The scaling factors of the density gradient ranged from 1/6 to 10. Figures 12 and 13 shows  $\gamma$  and  $\omega$  versus  $k_\perp \rho_s$  and Figures 14 and 15 show the maximum  $\gamma$  and corresponding  $\omega$  as functions of the scaling factor of the density gradients.

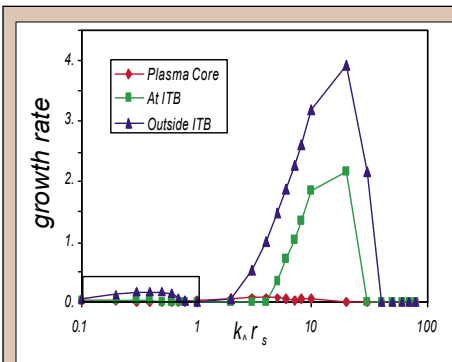


Figure 5. Growth rates of ITG, TEM, and ETG drift wave modes as a function of normalized wave vector, for the three regions of interest.

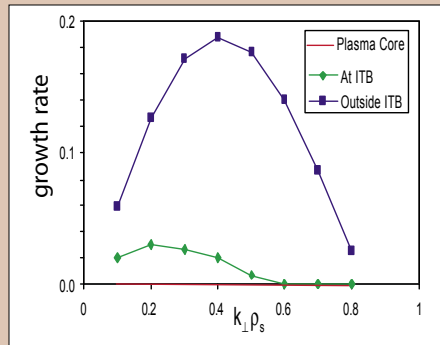


Figure 6. ITG growth rate as a function of normalized wave vector, for three regions in the plasma.

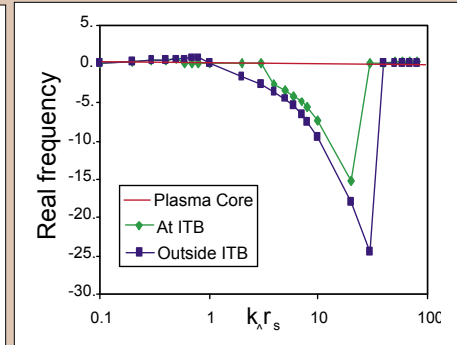


Figure 7. ITG, TEM, and ETG real frequencies as a function of normalized wave vectors at three regions in the plasma.

## DISCUSSION AND CONCLUSIONS

### A. Instabilities in Three Regions of the Plasma

GS2 solutions of the gyrokinetic equation were examined for drift wave instability, that is, a positive growth rate. If the simulated modes are stable, then no transport would be driven by these modes. All drift wave modes were stable in the plasma core (Figure 5) [6, 7]. In the ITB region, however, the ITG is unstable, which could cause some transport of heat and particles. However, Figure 5 shows that the ITG instability in the barrier region is significantly weaker than that found outside the ITB. This is likely the cause of the developing good confinement (i.e., lack of transport) within the barrier. There are also strong ETG instabilities both at and outside the ITB, but because the ETG has the shortest wavelengths of the drift wave modes, it is unlikely that it will have much effect on ion transport. ETG is thought to be important in heat transport mediated by electrons.

### B. At the ITB Region: Temperature Gradient Scaling

Figure 10 indicates that at small normalized temperature gradients, the ITG is stable in the ITB region until the temperature gradient reaches a critical value, then it becomes approximately linearly unstable. The bump in the linear region of the graph, which corresponds to the dip in Figure 11, is due to the fact that the value of  $k_{\perp}\rho_s$  at which the maximum growth rate occurs changes from 0.2 to 0.3, as can be seen in Figure 8. The simulation's critical temperature gradient is 0.80 of the experimental value. Thus, the experiment is well above marginal stability; recall that the ITG was found to be unstable in this region (Figure 6).

### C. At the ITB Region: Density Gradient Scaling

The GS2 simulations showed that the ITG growth rates cannot be made zero in the barrier region by scaling the normalized density gradients (Figure 14). The growth rate has a relatively weak

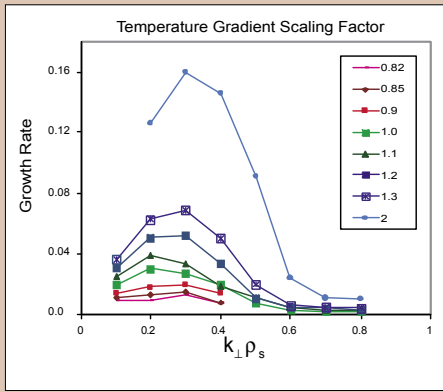


Figure 8. ITG growth rates at the ITB region.

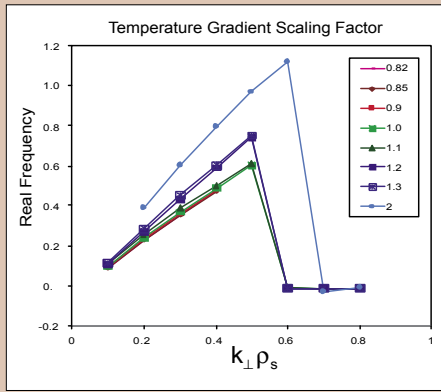


Figure 9. ITG real frequencies at the ITB region.

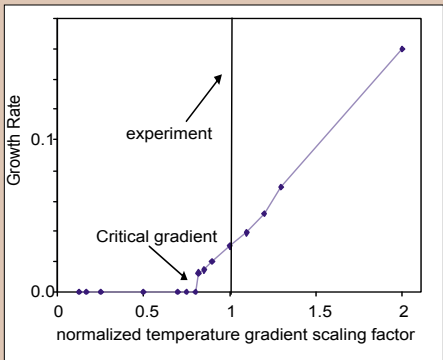


Figure 10. ITG growth rate as a function of normalized temperature gradient.

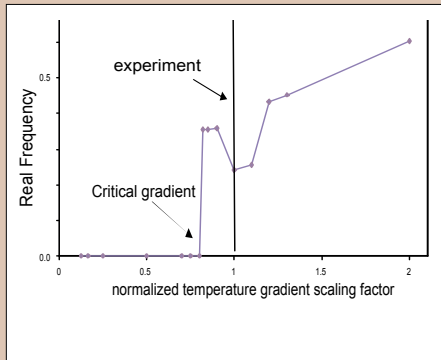


Figure 11. ITG real frequency as a function of normalized temperature gradient.

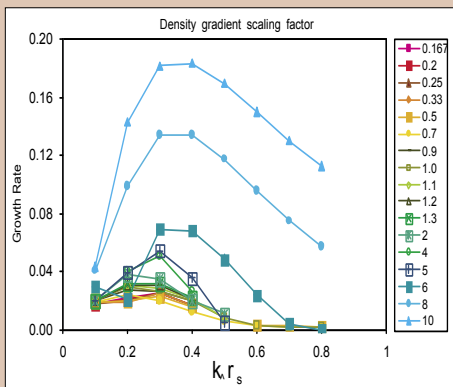


Figure 12. Drift wave mode growth rates at the ITB region.

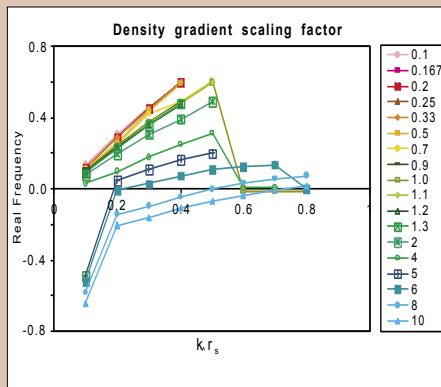


Figure 13. Drift wave mode real frequencies at the ITB region.

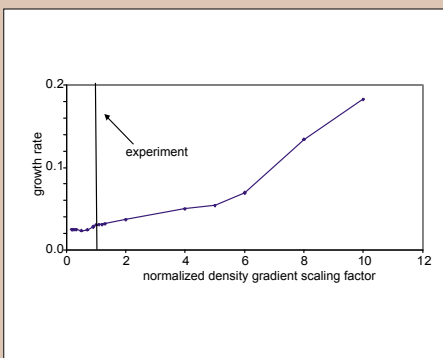


Figure 14. Drift wave mode growth rate as a function of normalized density gradient.

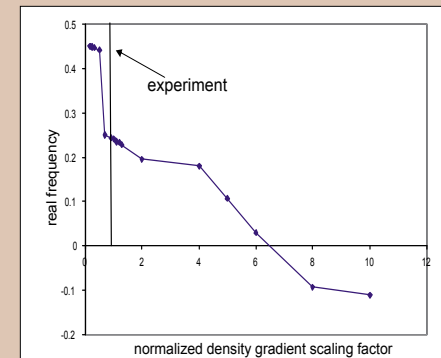


Figure 15. Drift wave mode real frequency as a function of normalized density gradient.

dependence on normalized density gradient—the experimental gradient had to be scaled by a factor of ten to increase the growth rate by a factor of about nine, as opposed to the temperature gradient, which only had to be scaled by a factor of two to increase the growth rate by a factor of eight.

There is a transition in the character of the most unstable ITG range drift waves as the normalized density gradient increases. Compare the real frequencies as a function of scaling factor in Figure 15 with the real frequencies for our base cases of ITG, TEM, and ETG modes in Figure 7. The most unstable drift wave starts as an ITG mode, but then shifts to a TEM mode at about 6.5 times the normalized experimental density gradient, as seen by the real frequency becoming negative and a development of discontinuity in the slope of the growth rate. This is to be expected from the stability diagram in Figure 16, showing the effects of the temperature and density gradients on drift wave instability [8]. A high enough shift in the normalized density gradient changes the mode from ITG to TEM.

In conclusion, it was found that at the barrier region, just before ITB onset, transport is likely caused primarily by weak instabilities of the ITG, the drift wave mode of longest wavelength. Transport can be further reduced by decreasing the species' temperature gradients, which stabilizes the ITG. In addition, increasing the density gradients will induce a shift from the ITG to a potentially less dangerous mode at shorter wavelength, the TEM, which may also reduce ion transport. Nonlinear simulations are needed to verify these conclusions.

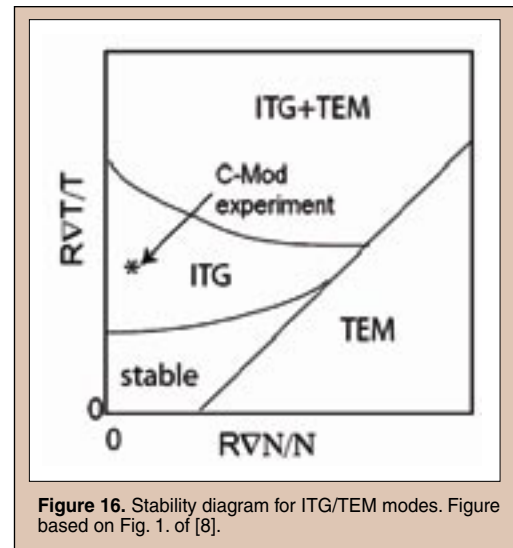


Figure 16. Stability diagram for ITG/TEM modes. Figure based on Fig. 1. of [8].

Much of the study described here will appear in a forthcoming publication [7].

### FUTURE RESEARCH

Many lines of future research would be interesting. For example, future research could include investigation of marginal stability conditions in the plasma core and outside the ITB region, as well as the effect on the critical temperature of density and temperature perturbations for each species separately. Critical gradients can be compared to standard models [9]. In addition, nonlinear ITG studies in the barrier region would deepen our understanding of ITB formation; shifts in critical temperatures have been found from nonlinear microturbulence studies[10].

### ACKNOWLEDGEMENTS

We would like to thank the U.S. Department of Energy and the Princeton Plasma Physics Laboratory for the opportunity to participate in the SULI program. We thank James Morgan for his enthusiastic and energetic work with the SULI students, and the Alcator C-Mod group at MIT for the data and analysis of the experiment. Work also supported by U. S. DOE Contract DE-AC02-76CH03073.

### REFERENCES

- [1] I. H. Hutchinson, R. L. Boivin, F. Bombarda *et al.*, Phys. Plas. 1, 1511 (1994).
- [2] J. A. Wesson, *Tokamaks*, Oxford University Press, New York, NY (1997).
- [3] C. L. Fiore, *et al.* Phys. Plas. 8, 2023 (2001).
- [4] M. Kotschenreuther, *et al.*, Comp.Phys. Com. 88, 128

Parameter	r/a=0.25	0.45	0.65
q	0.99	1.32	2.00
$\hat{s}$	0.51	0.96	1.48
$T_d/T_e = T_i/T_e$	0.99	1.16	1.06
$T_i/T_e$	1.30	3.96	1.59
$-a_{ref} \nabla n_i/n_e = -a_{ref} \nabla n_i/n_s$	0.71	0.42	0.04
$-a_{ref} \nabla T_i/T_e$	1.47	2.35	2.83
$-a_{ref} \nabla T_d/T_e = -a_{ref} \nabla T_i/T_e$	0.67	2.75	3.41
$-a_{ref} \nabla T_i/T_h$	-3.13	15.4	5.69
$v_e a_{ref}/(c_s \sqrt{2})$	0.30	0.56	1.54
$v_d a_{ref}/(c_s \sqrt{2})$	0.01	0.02	0.05
$v_b a_{ref}/(c_s \sqrt{2})$	0.07	0.11	0.33
$v_h a_{ref}/(c_s \sqrt{2})$	0.01	0.01	0.04
$T_{ref}(\text{keV})=T_e$	1.15	0.77	0.45
$n_{ref} = n_e (m-3)$	3.1x1020	2.8x1020	2.7x1020
$\beta_{ref}$	0.75%	0.45%	0.25%
Freq norm= $(T_{ref}/m_{ref})0.5/a_{ref}$ (sec-1)	1.07x106	0.88x106	0.67x106

**Table I.** Plasma parameters for C-Mod simulations at 0.9 sec. q is the safety factor,  $\hat{s}$  is the magnetic shear,  $T_s$  are the species (electron, deuteron, hydrogen, and boron) temperatures,  $n_s$  are the species densities,  $\nabla T_s$  are the species temperature gradients,  $\nabla n_s$  are the species' density gradients,  $v_s$  are the species collisionalities in units of  $c_s \sqrt{2}/a_{ref}$ , where  $a_{ref}$  is a reference length and  $c_s$  is the sound speed,  $\beta_{ref}$  is a reference beta,  $T_{ref}$  is a reference temperature,  $n_{ref}$  is a reference density, Freq norm is a frequency normalization. The ratios of densities are:  $n_d/n_e=0.8$ ,  $n_b/n_e=0.03$ ,  $n_h/n_e=0.04$ , and  $a_{ref}=0.22m$ .

(1995).

- [5] R. J. Hawryluk, in *Physics of Plasmas Close to Thermonuclear Conditions*, edited by B. Coppi, G. G. Leotta, D. Pfirsch, R. Pozzoli, and E. Sindoni (Pergamon, Oxford, 1980), Vol. 1, p.19.
- [6] M. H. Redi, *et. al.* EPS-2004, London, UK, paper P2-163.
- [7] M. H. Redi, *et. al.* "Microturbulent drift mode stability of before internal transport barrier formation in the Alcator C-Mod radio frequency heated H-mode", *Physics of Plasmas* (2005).
- [8] X. Garbet, P. Mantica, C. Angioni, *et al.*, "Physics of Transport in Tokamaks", to appear in Proceedings of the 31th EPS Conference on Plasma Physics and Controlled Fusion, London, England (2004), and *Plasma Physics and Controlled Fusion* (2005).
- [9] F. Jenko, W. Dorland, G. W. Hammett, *Phys. Plas.* **8**, 4096 (2001).
- [10] A. M. Dimits, G. Bateman, M. A. Beer *et al.*, *Phys. Plasmas* **7**, 969 (2000).